Low-Thrust Mission Analysis Using an Analytical Trajectory Optimization Model

P. M. LION* AND A. L. KORNHAUSER†
Princeton University, Princeton, N. J.

AND

G. A. HAZELRIGG JR.‡
General Dynamics, San Diego, Calif.

This paper uses an Analytic Trajectory Optimization Model (ATOM) to develop efficient computational techniques for the use in the early phase of low-thrust mission analysis. The validity of the expression for burning time from ATOM is extended over the full acceleration range, from impulsive to continuous burning. The computational techniques are demonstrated in two problems: 1) the selection of propulsion system parameters for maximum payload and 2) the optimization of the "mix" of high-thrust chemical boost and low-thrust electrical propulsion.

Introduction

DEVELOPMENT of electric propulsion system hardware has reached the point where the feasibility of these systems for primary spacecraft propulsion has been established. Determination of their future role, however, depends as much on software technology as on hardware technology. Indeed, at the present time, software may be the pacing item. A crucial need in the early phase of mission analysis is for computational techniques and programs that are capable of generating large amounts of data economically and with sufficient accuracy to study basic mission design and spacecraft tradeoffs. For chemical rockets, such programs, based on the impulsive or ballistic approximation, are available; for low thrust systems, trajectory calculation is more difficult and the interaction with vehicle parameters more complex. In Refs. 1–3, an Analytic Trajectory Optimization Model (ATOM) is developed which, as its name implies, uses an approximate analytic solution to simulate low-thrust trajectories. With this solution, the numerical integration of trajectories can be eliminated for preliminary mission analyses, and the resulting computing times are equivalent to those required for impulsive trajectories. Accuracy is well within that required for preliminary analysis.

In this paper, ATOM is reviewed briefly with an emphasis on its role in the mission analysis process. In addition, an improvement in the expression for the burn time given in Refs. 1 and 2 is presented, which extends the validity over the full acceleration range, from impulsive to continuous burning. The use of ATOM in mission analysis is demonstrated for two problems: 1) the selection of propulsion system parameters for maximum payload and 2) the optimization of the "mix" of high thrust-chemical boost and low-thrust electric propulsion. Analytic results are compared with numerical solutions from an integration-optimization program and agree within 5% for the missions considered.

Presented as Paper 70-96 at the AIAA 8th Aerospace Sciences Meeting, New York, January 19–21, 1970; submitted March 6, 1970; revision received July 29, 1970. The Analytical Methods of Trajectory Analysis research is supported by the Office of Space Science and Applications, NASA Headquarters under NASA Grant NGR 31-001-152. J. W. Haughey is the NASA Program Monitor, and W. E. Miner, NASA Electronic Research Center, was Technical Monitor. The work made use of computer facilities supported in part by the National Science Foundation Grants NSF-GJ-34 and NSF-GU-3157.

* Associate Professor. Member AIAA.
† Graduate Student.
‡ Staff Scientist, Convair Division. Member AIAA.

Modeling of Vehicle Mass Components

In order to perform the mission analysis, it is necessary to model the various mass components which comprise the vehicle. The payload mass can be expressed in terms of the component masses of the spacecraft: $m_n = m_0 - m_p - m_{ps} - m_t$, where m_n = payload mass, m_0 = initial mass, m_p = fuel mass, m_{ps} = propulsion system mass, and m_t = tankage mass. A common convention is to assume the tankage mass proportional to fuel; i.e., $m_t = k_t m_p$. Using this assumption, the expression for payload mass becomes

$$m_n = m_0 - m_p(1 + k_t) - m_{ps} \tag{1}$$

Thus there are three components of mass for which mathematical models must be developed.

The first of these is the initial mass which is primarily a function of the hyperbolic excess velocity provided by the chemical launch vehicle

$$m_0 = m_0(v_h) \tag{2}$$

Mathematical models for various launch vehicles have been developed and are usually presented in graphical form.[4] Figure 1 shows a curve for the SIB/Centaur.

The second mass component which must be modeled is the propulsion system mass. m_{ps} is a function of the initial thrust acceleration a_0 (initial thrust/mass ratio) and the jet exhaust velocity v_j (or, equivalently, specific impulse):

$$m_{ps} = m_{ps}(a_0, v_j) \tag{3}$$

Although there are many parameters involved in the design of a nuclear electric propulsion system, the only parameters which affect propellant consumption are a_0 and v_j; all other parameters should be chosen to minimize m_{ps}.

Modeling the propulsion system mass accurately over a wide range of parameters is a difficult task and much research remains to be done. A common, simplified model assumes that propulsion system mass is proportional to raw power at the terminals of the power supply:

$$m_{ps} = \alpha P$$

and thus

$$m_{ps} = \alpha a_0 v_j / 2\eta \tag{4}$$

where η is an efficiency factor. At any rate, the ATOM can be used with either the simplified model or more realistic models as they become available.

The analytic solution developed in this paper is a mathematical model of the propellant mass expended on a trajectory in which the thrust-time history has been optimized (to minimize propellant). By using only optimum thrust programs, the propellant mass is reduced to a function of three variables§:

$$m_p = m_p(v_h, a_0, v_j) \tag{5}$$

In addition to the function itself, the derivatives $\partial m_p/\partial v_h$, $\partial m_p/\partial a_0$, and $\partial m_p/\partial v_j$ can be determined. These derivatives are necessary when one desires to determine the propulsion parameters to maximize the payload.

In the past it has been necessary to numerically integrate trajectories to determine m_p for each set of values of a_0, v_h, v_j. Over the range in which ATOM is valid, one can determine m_p (and its derivatives) for all values of these propulsion parameters by finding the optimal impulsive trajectory and solving a set of matrix equations; thus, all trajectory integration can be eliminated which, in turn, can save an enormous amount of computer time.

Equations of Motion and Necessary Conditions

Three distinct cases are considered in the development of the solution. In order of decreasing analytic complexity, they are 1) bounded thrust, 2) bounded acceleration, and 3) impulsive.

The equations of spacecraft motion for the bounded-thrust case can be written

$$\ddot{\mathbf{r}} = \mathbf{g}(\mathbf{r}) + F\mathbf{v}/m \qquad \dot{m} = -F/v_j \tag{6}$$

where $\mathbf{g}$ is the gravity vector, F is the thrust magnitude, $\mathbf{v}$ is a unit vector in the thrust direction, and v_j is the jet exhaust velocity. Since the thrust is bounded, we have $0 \leq F \leq a_0 m_0$, where a_0 is the initial thrust-acceleration. Necessary conditions for an optimal trajectory are stated in terms of the adjoint vector. The differential equations for the adjoint vector can be written

$$\ddot{\lambda} = G\lambda \qquad \dot{\sigma} = T_p/m^2 \tag{7}$$

where ψ is the "primer vector" (the adjoint variables associated with velocity) and σ is the adjoint variable associated with mass. $p = |\lambda|$ is the magnitude of the primer vector. In terms of the switch function S, $S = p - \sigma m/v_j$, the necessary conditions are

$$F = a_0 m_0 \text{ if } S > 0 \text{ (maximum thrust)} \qquad F = 0 \text{ if } S < 0 \text{ (coast)} \tag{8}$$

The thrust direction must be aligned with the primer vector

$$\mathbf{v} = \psi/p \tag{9}$$

The bounded-acceleration case can be thought of as the limiting case of a bounded thrust as $v_j \to \infty$. In this case, the optimization criterion can be written as

$$\int_{\tau_b} a\,dt$$

where τ_b is the burn time. Mass need not be included as a state variable. This is a very useful approximation for low-thrust systems which have high exhaust velocity and in which the mass is, indeed, almost constant. Secondly, since it involves only one propulsion parameter, the maximum acceleration (a_0), the solution is more tractable and provides a convenient step toward the more difficult bounded-thrust case. The equations of motion are

§ Or four variables if a chemical retro is used for capture.

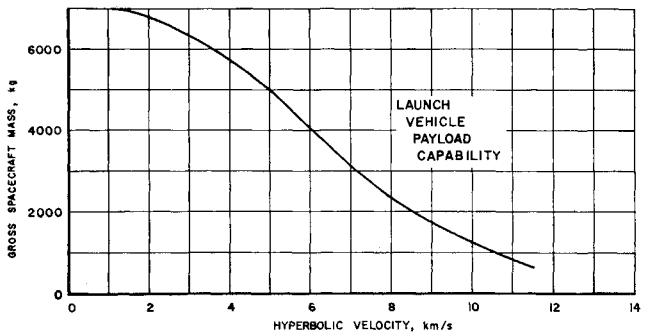

Fig. 1 Launch characteristics of the SIB/Centaur.

$$\ddot{\mathbf{r}} = \mathbf{g}(\mathbf{r}) + a\mathbf{v} \tag{10}$$

where the thrust-acceleration is bounded, $0 \leq a \leq a_0$. The necessary conditions are analogous, and the switch function simplifies to

$$S = p - 1 \tag{11}$$

Thus

$$a = a_0 \quad p > 1 \text{ (maximum acceleration)} \tag{12a}$$

$$a = 0 \quad p < 1 \text{ (coast)} \tag{12b}$$

Again, the thrust-acceleration is aligned with the primer vector and the differential equations for the primer vector are the same as Eq. (7).

The impulsive case is the limit of both bounded-acceleration and bounded-thrust cases as $a_0 \to \infty$. The optimal control is now a series of velocity impulses and the optimal trajectory a sequence of intersecting conic arcs. The necessary conditions can again be stated in terms of the primer vector: at impulse points $p = 1$ and the impulse is applied in the direction of λ; at all other points $p < 1$. The differential equations for the primer are again given by Eq. (2). These necessary conditions are also the limiting case of those cited for the bounded-thrust and bounded-acceleration cases.

Form of the Solution

The approach used by ATOM is to develop the finite-thrust trajectory as a mathematical expansion about the optimal impulsive trajectory which satisfies the same boundary conditions.

In the case of bounded acceleration, both the position and primer vectors along the optimum finite-thrust trajectory are expanded in series in $1/a_0$:

$$x = x^{(0)} + x^{(1)}/a_0 + x^{(2)}/a_0^2 + \ldots \tag{13a}$$

$$\lambda = \lambda^{(0)} + \lambda^{(1)}/a_0 + \lambda^{(2)}/a_0^2 + \ldots \tag{13b}$$

Superscript 0 stands for the impulsive case, and superscripts 1, 2, etc. denote higher order corrections; thus, both x and λ approach their impulsive values as $a_0 \to \infty$.

In order to be able to meet the switching conditions on the magnitude of the primer vector, it is also necessary to expand each thrust interval in series:

$$\tau_k = (\Delta V_k/a_0) + (\tau_k^{(2)}/a_0^2) + \tau_k^{(3)}/a_0^3 + \ldots \tag{14}$$

where ΔV_k is the kth velocity impulse on the impulsive trajectory, $\tau_k^{(2)}$ and $\tau_k^{(3)}$ are corrections due to finite thrust time (from these corrections, the burn duration losses or so-called "gravity losses" can be calculated). Note that $\tau_k \to 0$ and $a_0\tau_k \to \Delta V_k$ as $a_0 \to \infty$.

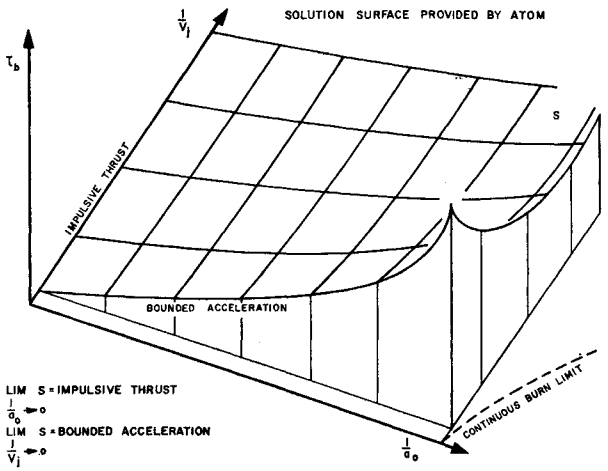

Fig. 2 S is the solution surface provided by ATOM.

The series (13) and (14) are substituted into the differential Eqs. (7) and (10) and the results made to satisfy the required boundary conditions. Integrating across each burn and then equating powers of $1/a_0$ produces a system of matrix equations for each power.

For the bounded-thrust case, the series corresponding to Eqs. (13) and (14) are expanded in terms of two variables, $1/a_0$ and $1/v_j$. For example, the expansion of the thrusting intervals takes the form

$$\tau_k = \frac{1}{a_0}\left(\Delta V_k + \frac{1}{v_j}\tau_k^{(1,1)} + \frac{1}{v_j^2}\tau_k^{(1,2)} + \ldots\right) + \frac{1}{a_0^2}\left(\tau_k^{(2,0)} + \frac{1}{v_j}\tau_k^{(2,1)} + \ldots\right) + \ldots \quad (15)$$

There are no terms of the form $1/v_j^k$, since the solution must approach the impulsive case as $a_0 \to \infty$ irrespective of the value of v_j. As $v_j \to \infty$, the solution approaches the bounded-acceleration case. Indeed, the terms in $1/a_0^k$ are the same as in the bounded-acceleration case; i.e., $\tau_k^{(2,0)} = \tau_k^{(2)}$ from Eq. (14), etc. Thus, solving the bounded acceleration case is included in solving the bounded-thrust case. Although there are more terms in the bounded-thrust case, the solution follows the same pattern as before. Full details appear in Ref. 2.

Once the expression for the total burn time $\tau_b = \Sigma_k \tau_k$ is known, the propellant mass fraction $\mu(= m_p/m_0)$ can be expressed in terms of a_0 and v_j: bounded-acceleration case;

$$\mu = 1 - \exp(-a_0\tau_b/v_j) \quad (16)$$

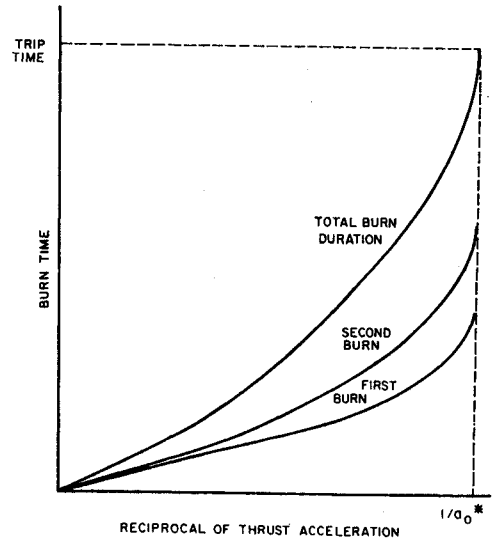

Fig. 3 Burn time vs reciprocal of thrust acceleration.

bounded-thrust case;

$$\mu = \dot{m}\tau_b = a_0\tau_b/v_j \quad (17)$$

A graphical representation of the solution given by ATOM is shown in Fig. 2. The total engine thrusting time is plotted (on the vertical coordinate) as a function of $1/a_0$ and $1/v_j$. The bounded-acceleration case is along the $1/a_0$ axis ($1/v_j = 0$); the impulsive case is along the $1/v_j$ axis ($1/a_0 = 0$). The latter is a "level line," since the impulsive solution is independent of v_j.

An Improved Expression for the Burn Time

The accuracy of the ATOM is best for high thrust levels, since it is an expansion about the impulsive case. Accordingly, one would expect the accuracy to decrease for lower thrust levels. Indeed it does, however, a slight modification can be made in the expression for burn time (τ_b) that greatly improves its accuracy at low thrust levels.

For the case of constant thrust acceleration, a sketch of total burn time vs $1/a_0$ is shown in Fig. 3. T is the prescribed total trip time and a_0^* is the thrust level corresponding to continuous burning. The important thing to note is that the slope of the curve is infinite at $1/a_0^*$. A polynomial such as Eq. (14) cannot describe this behavior (unless an infinite number of terms are used).

Much insight can be obtained by considering the problem of a one dimensional fixed-time transfer between two points in field-free space such that the velocity at each terminal point is zero. If the distance between the two points is d and the prescribed transit time is T, then the total impulsive velocity increment is $\Delta V = 2d/T$. The velocity profile is shown in Fig. 4a. If the thrust-acceleration is bounded the velocity profile is as shown in Fig. 4b; it is necessary to accelerate to a higher velocity in this case to make up for the finite burning time.¶ The expression for the velocity increment in this case is

$$\Delta V_a = 2\Delta V_\infty/1 + (1 - 2\Delta V_\infty/a_0T)^{1/2}$$

where a_0 is the magnitude of the thrust-acceleration. The expression for the burn time can be written

$$\tau_b = T[1 - (1 - \Delta V_\infty/a_0T)^{1/2}] \quad (18)$$

where ΔV_∞ is the impulsive velocity increment and T is the transit time. The lowest value of thrust-acceleration, which will accomplish the transfer in the prescribed transit time, is $a^* = 2\Delta V_\infty/T$. The corresponding velocity profile is shown in Fig. 4b. When the expression for τ_b [Eq. (18)] is plotted

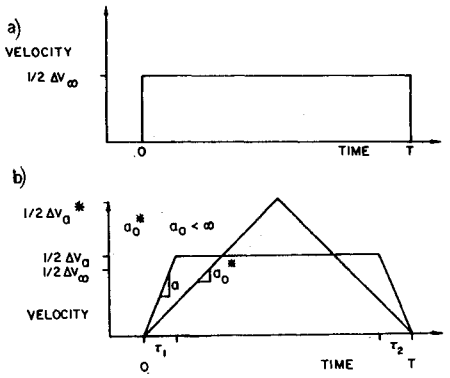

Fig. 4 a) One-dimensional, field-free impulsive thrust and b) one-dimensional, field-free finite thrust.

¶ This is the real source of what are known as "gravity losses." Since they occur in field-free space, a better term would be "burn duration losses."

vs $1/a$, a curve of the form shown in Fig. 3 results, including the infinite slope at $1/a^*$.

By analogy with the field-free case, it is assumed that the total burn time can be written in the form

$$\tau_b = T\left[1 - \left(1 - \frac{1}{a_0}T^{(1)} + \frac{1}{a_0^2}T^{(2)} + \ldots\right)^{1/2}\right] \quad (19)$$

for the bounded-acceleration case, and

$$\tau_b = T\left[1 - \left(1 - \frac{1}{a_0}\left[T^{(1,0)} + \frac{1}{v_j}T^{(1,1)} + \ldots\right] + \frac{1}{a_0^2}\left[T^{(2,0)} + \ldots\right] + \ldots\right)^{1/2}\right] \quad (20)$$

for the bounded-thrust case. The coefficients $T^{(0,1)}$, $T^{(1,1)}$ etc. are determined by fitting the curve defined by Eq. (19) or Eq. (20) to that defined by Eq. (15) at the point $1/a_0 = 0$, where $\tau_b = 0$, and all the derivatives with respect to a_0 and v_j are known.

Even with a finite number of terms, the expressions (19) and (20) have the correct behavior at $1/a_0^*$, where the appropriate value of $1/a_0^*$ is the smallest positive root of

$$1 - (T^{(1,0)} + T^{(1,1)}/v_j)/a_0^* \ldots - (T^{(2,1)} \ldots)/a_0^{*2} = 0 \quad (21)$$

The corresponding expression would be used for the constant-acceleration case.

It should be recognized that the actual curve of τ_b vs $1/a_0$ does not have exactly the square root behavior predicted by Eqs. (19) and (20). Likewise, the value of $1/a_0^*$, which results from solving Eq. (21), is an approximation. However, in the cases examined so far these have proved to be extremely good approximations and represent a vast improvement over Eq. (15). In these cases this technique has resulted in an error in total time of less than 4% at the continuous burning acceleration ($1/a_0^*$) for large values of v_j. The error is defined as the difference between the ATOM solution and a solution from a numerical integration program. The error is substantially reduced as a_0 is increased. Typical results are shown in Fig. 5 where percent error in total burn time is plotted vs $1/a_0$ for a 192-day, 135° Earth-Mars transfer (bounded acceleration).

Similar results for a bounded-thrust case are shown in Fig. 6. Here contours of constant error in burn time are plotted on a $1/v_j - 1/a_0$ map for the same mission as used in Fig. 5. The difference between Eq. (20) and the numerical solution is shown in solid contours; the difference between Eq. (15) and the numerical solution is shown in dashed contours. Notice that the accuracy of ATOM has been extended to higher values of $1/a_0$.

Perhaps the most important improvement resulting from this technique is the increased accuracy with which the derivative $\partial\mu/\partial a_0$ can be determined. This is an important derivative in optimizing payload as will be seen in the following section. Using Eq. (15), the accuracy in $\partial\mu/\partial a_0$ is comparable to that of $1/a_0^*$. In Fig. 7 a comparison of $\partial\mu/\partial a_0$ as calculated by using the power series solution, the improved technique and the numerical solution is shown for the Earth-Mars mission previously discussed.

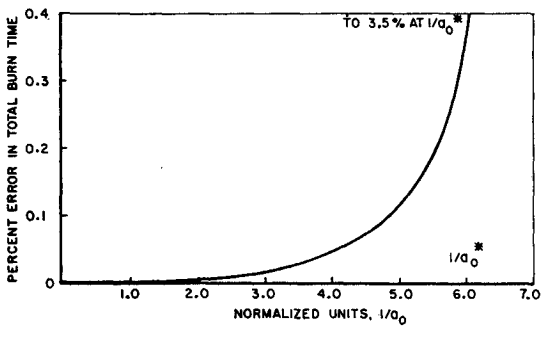

Fig. 5 Error in total burn time (Earth-Mars transfer 192-days, 135°, $V_j \rightarrow \infty$).

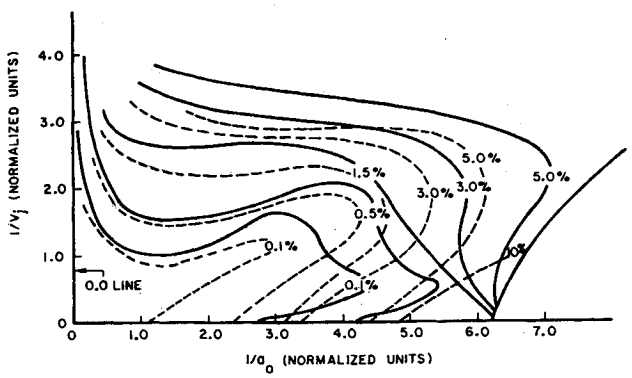

Fig. 6. Difference between ATOM and a numerical integration solution of propellant mass requirements (Earth-Mars 192-Days, 135° coplanar rendezvous).

Applications

The usefulness of the analytic solution for preliminary design and mission optimization is a result of the analytic expressions for propellant mass fraction [Eqs. (16) and (17)]. The derivatives of μ with respect to a_0 and v_j are obtained by simply differentiating these expressions. The derivative of μ with respect to v_h is $\partial\mu/\partial v_h = p(0)$, where $p(0)$ is the magnitude of the primer vector at $t = 0$. (This expression, which depends upon proper scaling of the adjoint variables, can be derived from the transversality equation.)

In the examples which follow it should be noted that, when the analytic solution is applied to a given mission, results are obtained for all values of v_j and a_0 (within the range of validity of the solution). Although iteration is required to determine optimum values of these parameters, no recalculation of the trajectory is required. When v_h is included as one of the independent variables, it is necessary to iterate the solution of the adjoint vector and the ATOM matrix equations. A straightforward method of iteration is included in the Appendix. By contrast, using a numerical integration-optimization program, one must recalculate the entire trajectory for each set of values of a_0, v_j, and v_n.

The first example is the problem of determining the "mix" between high-thrust boost and low-thrust electric propulsion so as to maximize payload. Bounded acceleration is assumed for this example. Using the spacecraft mass model discussed

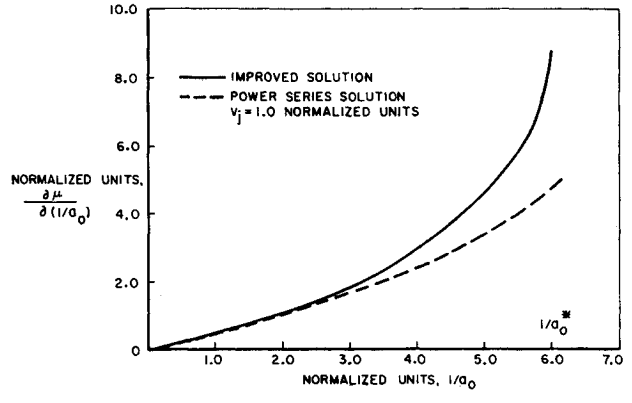

Fig. 7 Derivative of propellant mass requirement.

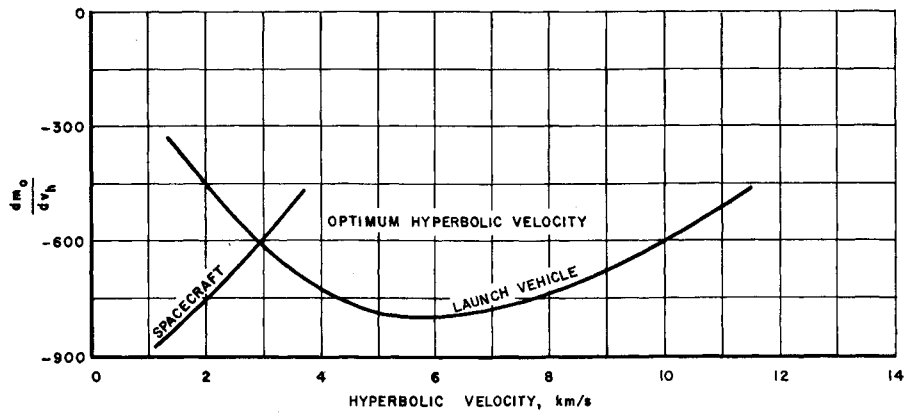

Fig. 8 Graphical solution for finding optimum V_h.

previously,

$$m_n = m_0\, 1 - \mu(1 + k_t) - \alpha P/\eta \qquad (22)$$

It hs been assumed that $m_{ps} = \alpha P/\eta$ and the power level (P) and efficiency (η) are given.

The problem is to determine the value of the hyperbolic excess velocity (v_h) (i.e., the amount of high-thrust boost) which maximizes the payload m_n. m_0 is a function of v_h as given by a launch vehicle capability curve (e.g. Fig. 1 for the Saturn 1B/Centaur). The propellant mass fraction for the low-thrust system (μ) is also a function of v_h. The optimum value of v_h is determined by setting the derivative of Eq. (22) equal to zero, giving

$$\nu\, \partial m_0/\partial v_h = m_0\, (1 + k_t)\, \partial\mu/\partial v_h \qquad (23)$$

where

$$\nu = [1 - \mu(1 + k_t) - k_s - (\alpha P/\eta)]$$

The derivative $\partial m_0/\partial v_h$ is determined from launch vehicle performance data. The only unknowns are μ and $\partial\mu/\partial v_h$ which are determined by ATOM.

Equation (23) is a nonlinear algebraic equation for v_h which can be solved graphically by the method of the Appendix. The solution for a 252-day Earth-Mars mission is indicated in Fig. 8. A performance curve, $\partial m_0/\partial v_h$, is plotted for the Saturn 1B Centaur and, on the same grid, a line representing $m_0/\nu(1 + k_t)\partial\mu/\partial v_h$. The intersection of these curves is the solution of Eq. (23). Table 1 summarizes the results.

The second example is the optimization of two propulsion parameters, a_0 and v_j, for maximum payload, in the constant thrust case. Here, v_h is assumed fixed so that maximization of the payload fraction (ν) is the same as maximization of the actual payload. Payload fraction is written

$$\nu = 1 - \mu(1 + k_t) - P/m_0$$

The optimum values of a_0 and v_j are determined by simultaneous solution of the nonlinear equations, $\partial\nu/\partial a_0 = 0$, $\partial\nu/\partial v_j = 0$, where both the power level (P) and the propellant fraction (μ) are functions of a_0 and v_j:

$$\mu = \dot{m}\tau_b = a_0/v_j\, \tau_b \qquad P/m_0 = a_0 v_j/2\eta$$

Table 1 Optimization of v_h

Boundary conditions (two dimensions)	
Launch from Earth: Dec. 6, 1979	
Arrive at Mars: July 18, 1980	
$\eta = 0.6$ $k_t = 0.06$ $\alpha = 0.01$ kg/W	
$P/m_0 = 20$ W/kg $v_j = 30{,}000$ m/sec	a = 0.00133 m/sec^2
Impulse at Mars: 1906.1 m/sec	Optimum v_h (analytic) 3000 m/sec (numerical) 3014.7 m/sec
Percent difference 0.005%	

τ_b is determined as a function of a_0 and v_j from Eq. (21).

Table 2 compares the analytic results for a 192-day 135° Earth-Mars coplanar rendezvous mission to numerical results obtained from the TOPCAT Program.[4] The two methods differ by less than 3.5%. The analytic solution, however, required approximately two orders of magnitude less computer time.

The two examples previously stated can be combined to give an overall mission optimization with respect to electric propulsion parameters (a_0,v_j) and hyperbolic excess velocities (at arrival and departure).

Conclusions

Using the Analytic Trajectory Optimization Model (ATOM), low-thrust trajectories (of sufficient accuracy for preliminary analysis) can be calculated with computing times comparable to that of impulsive trajectories. A modification of the expression for total burn time (Eq. 20) increases the accuracy of ATOM so that it can be used over the full range of thrust levels, from impulsive to continuous thrusting.

Once the optimal impulsive trajectory has been found and the ATOM equations solved, analytic expressions for the propellant mass fraction and its derivatives with respect to a_0, v_h, and v_j are available. Also available are thrust pointing directions and thrust on-off switching times. Optimum values of the propulsion parameters can then be determined by the iterative solution of nonlinear algebraic equations. (The determination of the derivative $\partial\mu/\partial v_h$ does require resolving the adjoint vector and the ATOM matrix equations.)

The accuracy of these results has been found to compare favorably with the solution of a numerical integration program which requires far more computing time. Two examples are included to illustrate this.

Appendix

Varying the value of v_h, the hyperbolic velocity, changes the initial velocity increment on the impulsive trajectory and thus changes the adjoint vector and the ATOM matrix equa-

Table 2 Optimization of v_j and a_0

Boundary Conditions (two-dimensional Earth-Mars simulation)	
Trip time: 192 days	Travel angle: 135°
$\eta = 1.00$, $k_t = 0.0$, $\alpha = 0.01$ kg/W	
Impulse at Earth: 3,835 m/sec	Impulse at Mars: 3,250 m/sec
Optimum a_0 (analytic)	$1.142\ 10^{-4}\ g$
(numerical)	$1.015\ 10^{-4}\ g$
Percent Difference	3.23%
Optimum v_j (analytic)	38,140 m/sec
(numerical)	37,831 m/sec
Percent Difference	0.82%

tions. For optimality, it can be shown that it is necessary that v_h be directed in the direction of the initial primer vector, $\lambda(0)$.

A simple procedure to allow variations in v_h follows:

1) Determine the optimum impulsive trajectory for $v_h = 0$. The initial velocity $\mathbf{v}(0) = \mathbf{v}_d(0)$, the orbital velocity of the departure planet.

2) Solve the impulsive adjoint equations and the ATOM matrix equations. (Analytic solutions for both are known.)

3) Optimize a_0 and v_j.

4) Compute the finite thrust value of $\lambda(0)$.

5) Based on the magnitude of $\lambda(0)$, estimate the optimal value of v_h.

6) Consider the initial velocity to be $v(0) = \mathbf{v}_d(0) + v_h \lambda(0)/p(0)$.

7) Return to step 2 and repeat until convergence is obtained.

References

[1] Hazelrigg, G. A. and Lion, P. M., "Analytical Determination of the Adjoint Vector for Optimum Space Trajectories," *Journal of Spacecraft and Rockets*, Vol. 7, No. 10, Oct. 1970, pp. 1200–1207.

[2] Hazelrigg, G. A., Kornhauser, A. L., and Lion, P. M., "An Analytic Solution for Constant-Thrust, Optimal-Coast, Minimum-Propellant Space Trajectories," Presented at the XX IAF Congress, Mar del Plata, Argentina, Oct. 1969.

[3] Hazelrigg, G. A., "An Analytic Study of Multi-Burn Space Trajectories", Ph.D. thesis, Sept. 1968, Princeton Univ., Princeton, N.J.

[4] "Launch Vehicle Estimating Factors," Office of Space Science and Applications, Launch Vehicle and Propulsion Programs, Jan. 1970, NASA.

[5] Lion, P. M., Campbell, J. H., and Shulzycki, A. B., "TOPCAT—Trajectory Optimization Program Comparing Advanced Technologies," Aerospace Engineering Rept. 717s, March 1968, Princeton Univ., Princeton, N.J.

JUNE 1971 AIAA JOURNAL VOL. 9, NO. 6

An Approximate Method for Nonlinear Ordinary Differential Equations

TSAI-CHEN SOONG*

The Boeing Company, Seattle, Wash.

A general method is derived for solving problems related to nonlinear, ordinary differential equations with variable coefficients. It consists of subdividing the domain into small regions in which the governing nonlinear differential equation with variable coefficients is reduced to a nonhomogeneous, linear, ordinary differential equation with constant coefficients, one for each region. The solution of the original problem is then taken as the collection of the general solutions of all subdivisions. The arbitrary constants of the complementary solution associated with each region are used to satisfy both the continuity requirements at regional boundaries and the initial or end conditions. The particular solutions compensate for the difference between the desired nonlinear solution and the resulting linear complementary solution. Two versions of the present method are presented. One which is more accurate requires the preparation of a computer program ab initio for each problem treated while the other can be written as a subroutine for general applications. Both versions provide an approximate, continuous solution with accuracy comparable or possibly superior to some commonly used numerical methods. A nonlinear initial-value problem of time-dependent coefficients and a nonlinear deflection of a variable flexible ring were analyzed.

Nomenclature

$A(t)$ = time-dependent cross-sectional area of column
$A_{i,j}$ = deflectional amplitude, Eq. (57)
A_j, B_j = vibratory amplitudes, Eq. (24)
E = Young's modulus
$F(t)$ = deflection function, Eq. (5)
$I(t)$ = time-dependent moment of inertia
I_0 = moment of inertia at $t = 0$, Eq. (9b); also at $s = \pi/2$, Eq. (37)
K_1, K_3 = spring constants of nonlinear foundation, Eq. (53)
L = length of column fixed between ends
P = pulling force on ring, Fig. 2; also axial force, Eq. (53)
$P(t)$ = variable axial compressive load
P_E = Euler buckling load of column at time t
P_0 = initial axial load on column
R = radius of ring
T = period of oscillation, real time, Eq. (36)
a_j, b_j, c_j = constants, Eq. (22)
b = amplitude, Eq. (5); constant related to moment of inertia, Eq. (37)
$c_{i,j}$ = constant coefficients of differential equations, Eq. (55)
$g_{i,j}$ = functions, Eq. (60)
k = constant, Eq. (9a); also Eq. (39)
p = one-half of the pulling force on ring, $P/2$
$p_{i,j}$ = roots, Eq. (59)
$q_{i,j}$ = functions, Eq. (60)
r_0, r_i = outer and inner radii of cylinder, Eq. (34)
s = nondimensional circumferential length of ring, true length/R
$\bar{s}_j$ = midpoint value of s, $(s_j + s_{j-1})/2$
t = time
v = total number of intervals or subdivisions
w = additional deflection of beam-column, Eq. (53)
x = coordinate
y = lateral deflection, Eq. (1); dependent variable, Eq. (62)
β = ratio of inner and outer radii of cylinder, Eq. (13)
δ_h, δ_v = horizontal and vertical displacements of ring, Eqs. (51) and (52)

Received January 14, 1970; revsion received August 3, 1970. The author acknowledges the help of C. Li in the programing and computations of the results and of C. Felippa in useful discussions.

* Senior Specialist, Structures Staff, Commercial Airplane Group.